FUTA JEET Vol 12 Issues 1&2 December, 2018

Journal of Engineering and Engineering Technology

ISSN 1598-0271

School of Engineering and Engineering Technology,
The Federal University of Technology, Akure, Nigeria

Journal of Engineering and Engineering Technology

Corrosion Assessment of Sinter Duplex Stainless Steel Composites in Pineapple Juice Extract

***[1,2] Olaniran O., [1]Borode J.O., [1]Afolabi A.E. [2]Olubambi P.A. [3]Olaniran B.A. [2]Folorunso D.O.**

1 Metallurgical & Materials Engineering Department, Federal University of Technology, Akure, Nigeria
2 Applied Microscopy & Triboelectrochemical Research Laboratory, Tshwane University of Technology, Pretoria, South Africa
[3]Computer Communication Department, Texas Tech University, Lubbock Texas, USA.

A B S T R A C T

Corrosion behavior of sintered oxide dispersion strengthened duplex stainless steel composites in pineapple juice extract was investigated using weight loss and potentio-dynamic methods. The scope of the work includes investigations on the effects of alloying elements, grain growth inhibitors, varying reinforceing ceramics starting powders. The sinter oxide dispersion strengthened (ODS) samples were characterized, using a combination of varying analytical techniques; scanning electron microscopy (SEM) and x-ray diffractometer (XRD). Gravimetric method is based on weight loss measurement while potentio-dynamic polarization scanning was done using an autolab potentiostat (PGSTAT 204 computer controlled) using the general purpose electrochemical software (GPES) version 1.10. Potentio-dynamic polarization curves were collected by scanning the potential from -1.0 to +1.5 V against Ag/AgCl at a scan rate of 2.0 mV/s. All electrochemical measurements were performed at room temperature in naturally aerated solutions. It was also observed that corrosion rate by gravimetric and polarization scanning provides relatively the same trend of information. Corrosion pits originated from the residual pores and grow as a result of weakening effect by the environment. Inclusions of partially Stabilized Zirconia (PSZ) help prevent further growth of the pits.

Keywords:
Corrosion, Oxide Dispersion Strengthening (ODS), polarization, composite, sinter.

Introduction

The powder metallurgical method (PM) offers an efficient technique for the fabrication of metal–ceramic composites and provides a uniform distribution of particulates in the composites (Chawla and Chawla, 2006). There are many approaches to improve the properties of PM stainless steels. Two major approaches are of significant interest. The first is the reinforcement with selected additives while the second is the improvement on sintering techniques. According to Padmavathi, *et al*. (2007), there is considerable scope for improving the properties of powder metallurgy components through novel sintering techniques and/or by alloying additives.

The in-situ second-phase grain reinforcement method of improving stainless steel properties has attracted increasing interests owing to the highly thermal stability of the reinforced phase, the highly interfacial strength between matrix and reinforced phase, the widely uniform distribution of reinforced phase in the matrix, and the excellent mechanical property of the grain reinforcement nanocomposite materials (Chen and Zhou, 2009). Ceramic particles such as metal oxides, metal carbide, and metal nitrides can be added to improve the mechanical properties. The addition of different ceramic particulates to metal matrix can result in improved stiffness, creep, fatigue and wear resistance (Molins, *et al.,* 1992). However, this improvement can compromise the

Correspondence:
*oladayolaniran@gmail.com
Tel. +2348035001939

corrosion resistance of the stainless steel.

Corrosion includes the destruction of metals in all types of atmospheres and liquids and at any temperature (Lakhtin, 1987; Garcia, *et al*., 2007). All constructional metals corrode, thus the corrosion engineer's problem is the determination of the rate at which corrosion or oxidation occurs. The rate varies according to the metal and the corrosive environment from being so low, that the reaction may be regarded as not occurring to being so fast, that the reaction occurs with almost explosive violence. Whether corrosion is detrimental to the use of a particular metal in a specific environment will depend on many factors such as time of exposure, temperature, oxygen concentration of the environment, usage (Lakhtin, 1987; Garcia, *et al*., 2007).

There is always a compromise in the property of a material whenever there is any alteration in the composition or microstructure of the material. In this case, corrosion properties of stainless steels can be compromised while trying to alter other properties such as mechanical and thermal (Reddy *et al*., 2010) by the addition of ceramic reinforcement. Corrosion has always been found to be a major challenge in industries producing food juices. Although the locally fabrication of food processing equipment is a welcome development, the problem of food contamination remains worrisome; hence, this study. Pineapples are among the common crops grown in almost every tropical country. Its juices, though may be acidic, are extracted for different usage.

Duplex stainless steels find extensive applications in tools, dies, and wear-and high-temperature oxidation-resistant component in the chemical and mining industries. However, the usage of duplex stainless steel composites in many industries in Nigeria especially the automobile industry, chemical, mining as well as food processing industries is very low. This work is aimed at studying the corrosion behavior of duplex stainless steel composites in pineapple juice extract to determine its suitability in food processing industries especially juice factories

MATERIALS AND METHOD

The consolidations of the composites have been reported elsewhere (Olaniran et al., 2013. The sample compositions are presented in Tables 1 and 2 respectively for 2205 and 2507 composites.

Table 1: Mixing ratio of powders for sinter Duplex stainless steel 2205 (wt. %)

Sample no	2205	$ZrO_2(Y_2O_3)$	Cr		Ni
X	100	_	_		_
A1	99.50	0.5	0	_	_
A2	98.5	0.5	1	0.815	0.185
A3	97.0	1	2	1.63	0.37
A4	95.0	2	2	1.63	0.37
A5	95.0	3	2	2.44	0.36

Table 2: Mixing ratio of powders for sinter Duplex stainless steel 2507 (wt. %)

Sample no	2507	$ZrO_2(Y_2O_3)$	Cr		Ni
Y	100	_	_		_
B1	99.50	0.5	0	_	_
B2	98.5	0.5	1	0.78	0.22
B3	97.0	1	2	1.56	0.44
B4	95.0	3	2	1.56	0.44
B5	95.0	2	3	2.3	0.7

Microstructural Characterization

Scanning Electron Microscope (SEM) (JEOL JSM – 7600F with EDX attachment) was used to study the microstructure of the samples. Elemental analysis was done using an energy dispersive X-ray spectrometer. The specimens were cross-sectioned and prepared for examination.

Electrochemical Studies

Two set of test specimens of duplex Stainless Steel were prepared – a set for potentiostatic measurement and the other set for gravimetric (weight loss) measurement. The preparation involves cutting, grinding, polishing of the samples to be tested. A set of twenty four specimens were cut and prepared from the Duplex Stainless steel composite samples. Twelve specimens for gravimetric test while the remaining twelve (for potentio-dynamicic scan) were cold mounted. This will help to compare and validate the results obtained from both experiments.

Weight loss Measurement (Gravimetric)

After surface preparation, the required dimensions of the entire specimen were accurately measured using micrometer screw gauge. The data were used to calculate the specimen's surface area which was used for calculation of corrosion rate. The specimens for gravimetric test were also weighed using analytical balance. The specimens were then stored in a desiccator to prevent pre-interaction with the environment in preparation for exposure to the corrosion environment.

a. Potentio-dynamic Polarization Measurement

Potentio-dynamic polarization measurement was done with an autolab potentiostat (PGSTAT 204 computer controlled) using the general purpose electrochemical software (GPES) version 1.10 in the Department of Metallurgical and Materials Engineering,

Federal University of Technology, Akure. It consists of a three-electrode (working, counter and reference) electrochemical cell. The ODS composite, a platinum foil, and an Ag/AgCl electrode were used as working, counter, and reference electrodes respectively. The ODS samples for electrochemical measurements were prepared by attaching an insulated copper wire to one face of the sample using an aluminium conducting tape, and cold mounted in resin. The samples were then left to dry in air at room temperature. Here, we have the control specimen designated as X and Y for pure sinter 2205 and 2507 composites respectively. The other test specimens were labelled A1- B5, with 2205 composites designated as A-series and 2507 composites designated as B-series. Details are presented in Tables 1 and 2 respectively. The electrolytes used for this experiment was pineapple juice extract, to represent the real life environment. The tests were carried out at room temperature.

The Pineapple juice extract used as corrodent in this experiment was prepared by weighing 5 kg of pineapple fruit. The fruit(s) is thoroughly washed in water. It is then peeled, cut, blended and filtered to obtain the juice extract. The obtained juice is poured into plastic bottles. The active chemical ingredient of the juice extract was analyzed in the department if Industrial Chemistry of the federal University of Technology and is presented hereunder.

34mg/100g of ascorbic acids, organic acids (citric acid, malic acid, tartaric acid, 36-41mg/100g of water soluble vitamins {thiamine (B1), riboflavin (B2), niacin, ascorbic acid, 5.5-10.5% of carbohydrate (mainly fructose and glucose) water.

The pH of the resulting juices or slurries were measured and recorded. From this time onward the bottles containing the juice extract was kept refrigerated when not in use to stabilize the pH.

The sinter ODS composites were polished to 1000 grade, washed in water and degreased with acetone. Polarization measurements were carried out at room temperature (25 ± 1) with the Autolab potentiostat. The potentiodynamic polarization curves were collected by scanning the potential from -1.0 to +1.5 V against Ag/AgCl at a scan rate of 2.0 mV/s. Potentiostatic current-time measurements at constant anodic potential were carried out by stepping the potential of the sinter composite to +1000 mV versus Ag/AgCl.

Data were obtained after 60 minutes immersions in the test electrolytes when only open circuit potential (OCP) measurements were recorded. Following this is the polarization scan. The tests were repeated to determine the average.

RESULTS AND DISCUSSION

The sinter stainless steel MMCs obtained was characterized using scanning electron microscope (Figures 1 and 2). It was observed that they do not show any reaction between partially stabilized zirconia (PSZ) particles and binder phase. Influencing the structure and mechanical properties of the composite is the metal-ceramic interface according to Pagoumis and Lindroos as reported by Akhtar and Guo, 2008). Interface debonding is not found in the sintered material, reflecting the good wettability of DSS with PSZ particles (Liu et al., 1994). Homogeneous distribution of the reinforcing particles will ensure isotropic mechanical properties and uniform distribution of stresses in the composite (Akhtar and Guo, 2008).

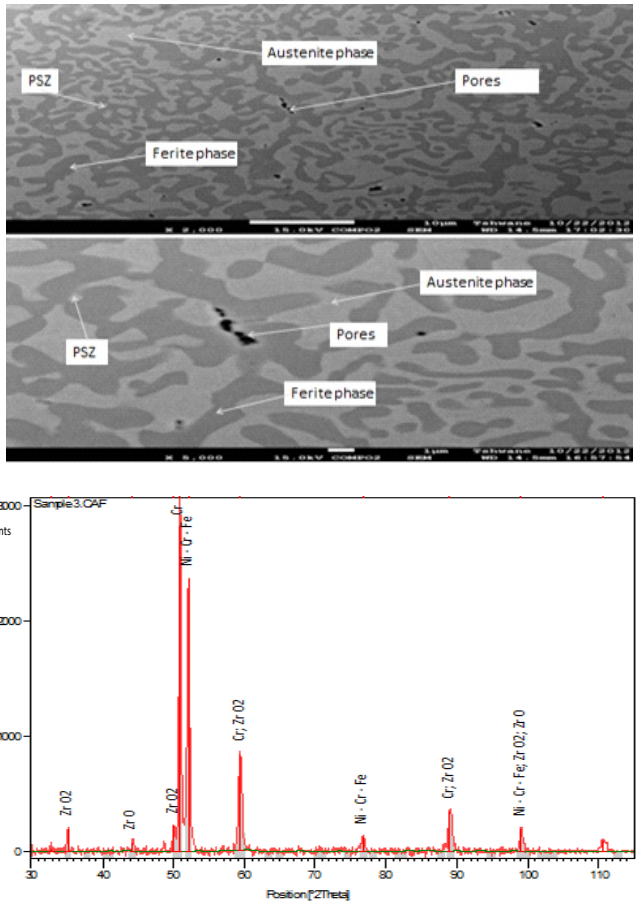

Fig. 1: Representative SEM micrograph of sinter 2205 composite at different magnification with the XRD.

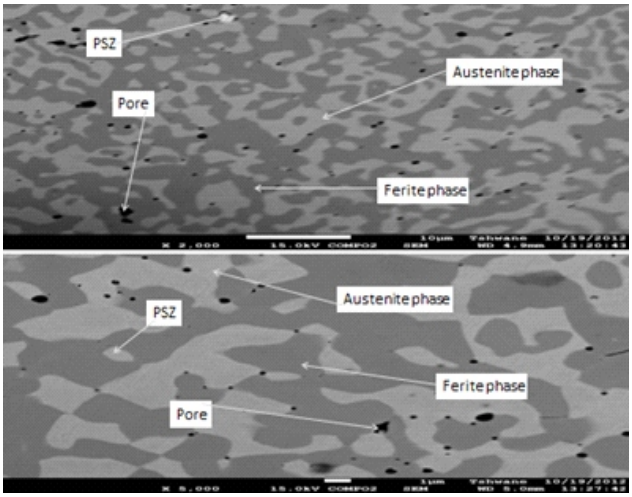

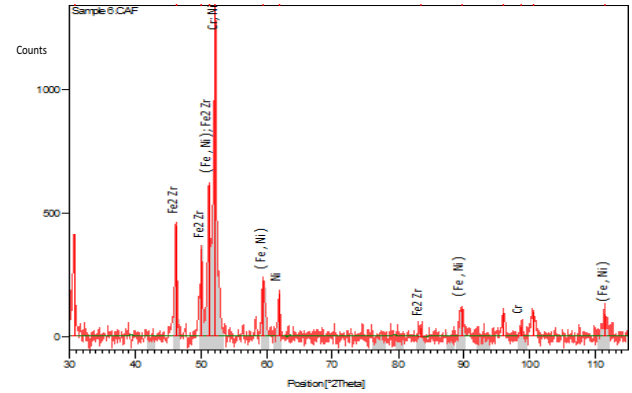

Fig. 2: Representative SEM micrograph of sinter 2507 composite at different magnification with the XRD.

The SEM results showed a heterogeneous microstructure of fairly large austenite grains with ferrite inter-grown. The sintered displayed a spare dispersion of the oxide particles in the matrix with the presence of some visible pores. The oxide inclusions were not distinctively seen as particle inclusions in the SEM images but shown in the XRD distinctive peak presented in section 4.6. This non distinctiveness in the SEM images could have resulted from the fact that during the hot consolidation processes by isostatic pressing, yttria and zirconia dissociated and dissolved into the matrix during sintering processes (Kim *et al*., 2008). PM steels usually possess residual porosity and heterogeneous microstructure, which arises from inhomogeneous of the participating powders (Liu *et al.,* 1994, Wei *et al*., 2002, Chawla and Chawla, 2006,). There were observations of pores in the SEM images of the sintered specimens. However, distributions and sizes differ which is one of the characteristics of sintered specimen from PM on the basis of their primary particle size (22 μ) and material desity.

Also, the reinforcement, PSZ, has different crystallographic orientations, as such, grain boundaries arise (Olaniran *et al*., 2012).

Introduction of chromium and nickel also have greater influence on the microstructure. Chromium, being a hard material, tends to resist compressibility upon application of external pressure. This also promotes residual porosity as observed in the SEM images (Chen *et al.*, 2007, Olaniran *et al*., 2017). The percentage pores sizes tend to increase with chromium addition. However, nickel addition on the other hand, due to its relatively lower melting point (1453°C), is capable of melting and possibly fill up the residual pores thereby reducing the pore shapes and sizes in the matrix and modifying the microstructures (Chen *et al*., 2007, Olaniran *et al.*, 2012). Further increase in the percentage composition of the reinforcement has shown further increment in the pores which confirmed the influence of nickel alloying on the microstructure of sintered duplex stainless steel composite (Olaniran *et al*, 2012).

The XRD results (Figures 1 and 2) showed that there was no existence of secondary phase other than bonding as a result of temperature increase so, the XRD diffractogram of the sintered 2205, 2507 and their composites show that the processing method used in this study did not encourage oxidation.

Although, X-ray diffraction can be very accurate in quantifying major components within a mixture, it may not be very good at detecting constituents that are present in trace amount. However, the XRD was able to pick all the dispersants present in the composites. Major phases which were clearly shown on the XRD include: MoC, MoNi, CrFeo, FeY, ZrO, FeCr, CrO, FeZr, Cr, ZrO, ZrO2, NiCrFe and NiY as indicated on the XRD analysis.

As indicated in Table 1, the Vickers hardness was obtained for the sintered samples. The hardness test was carried out under an indenter load of 0.1Hv and dwell time of 15 seconds. The influence of Ni addition was also observed on the hardness of the developed composites. It was expected that hardness should be increasing with increasing percentage of PSZ and Cr, which was actually observed from samples X and A1 in Fig. 3, Y and B1 in Fig. 4. But, the addition of Ni might have influenced the hardness such that addition of Ni has compromised the hardness for toughness (Muthupandi *et al.*, 2005, Younesi *et al.*, 2010, Olaniran *et al*., 2017, Obadele *et al*., 2017). This was evident in the hardness trend observed as the percentage composition of the Ni was increased with PSZ and Cr addition.

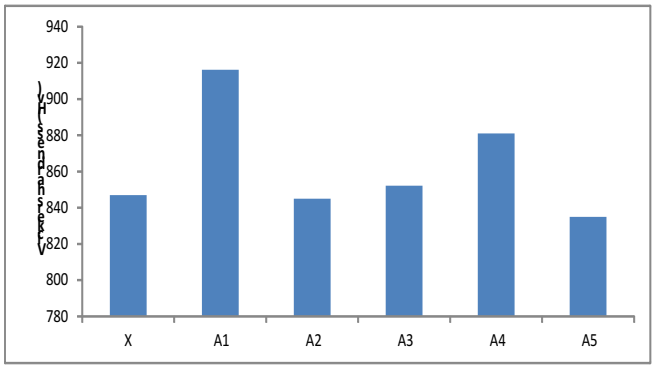

Figure 3: Vickers hardness of Sinter 2205 DSS Composites

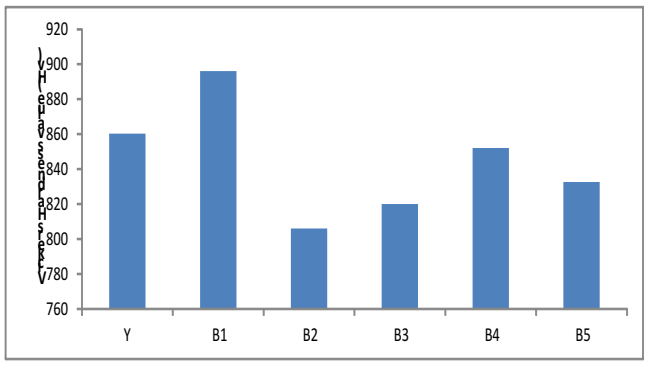

Figure 4: Vickers hardness of Sinter 2507 DSS Composites

GRAVIMETRIC MEASUREMENT

Results of weight measurements recorded at every four (4) days before and after were used to calculate the corrosion rate presented in Tables 3 and 4 for 2205 and 2507 composites respectively after exposure to the pineapple juice extracts for a period of 40 days. Figures 5 and 6 showed the corrosion rate against the exposure time in days. From the figures (5 and 6), all the 2205 composites displayed similar trend in the behaviour of the attack by the pineapple juice extract, that is, the corrosion rate continue to increase with the exposure time. The corrosion rate was noticed to be relatively lower between the first 20 days of exposure, which could be as a result of the materials moving from active to passive region, after which there was increase in the corrosion rate again. This could possibly be due to the change in the acidic level of the juice extract which has fallen from 4.3 to 3.3 as indicated in Table 4. However, on the general, the corrosion rates of the reinforced composites were much higher than that of the unreinforced 2205 (X) composites except for A3 that showed similar trend with the unreinforced. This could be connected to the presence of many grain boundaries created by the addition of the reinforcement which must have disturbed the lattice arrangement and also create many corrosion cites.

The corrosion rate of A1 is far higher than that of the unreinforced because of the change in the lattice/grain rearrangement by the addition of the reinforcement without a complimentary addition of Cr and Ni that could help lower the corrosion rate. However, the introduction of 0.49 % of Cr and 11 % Ni reduces the corrosion rate as indicated by plot A2 in figure 5. Further addition of Cr and Ni in A3 also brought down the corrosion rate in the juice extract but plot A4 and A5 which has the highest percentage of Cr and Ni addition can no longer reduce the corrosion rate despite the increase in the quantity added. In which case, the percentage chromium added is enough to convert the carbon to carbide; possibility is that there could be inadequate mixing of the 2205 matrix with the reinforcement, Cr nd Ni as reported by Olaniran *et al*., 2013. This was further confirmed by the plot of A5 which has the highest composition of Cr and Ni but yet the corrosion rate was the highest. This was possibly due to inadequate mixing.

Table 4: Variation of pH with days

Exposure time (days)	pH of Pineapple
0	4.3
4	4.1
8	3.9
12	3.6
16	3.4
20	3.3
24	3.1
28	3.0
32	2.8
36	2.5
40	2.3

The introduction of reinforcement and some other additives (Cr and Ni) as shown in Figure 6 for 2507 composites also shifted the corrosion rate in the positive region depending on the percentage of the reinforcement and other additives. This behaviour has been found to be as a result of disturbances and rearrangement of the lattices of the matrix by the additives. The degree of which was controlled by the amount of the additives and the homogeneity of the mix. B1 which has a smaller amount of reinforcement has increase in the corrosion rate compare to the sinter pure but addition of Cr and Ni to the same amount of PSZ brought down the corrosion rate as shown by the plot B2, However, further addition of reinforcement increase the corrosion rate despite further addition of Cr and Ni which could also be as a result of inhomogeneity of the powder mix for sintering as indicated by B4 with the highest percentage of reinforcement.

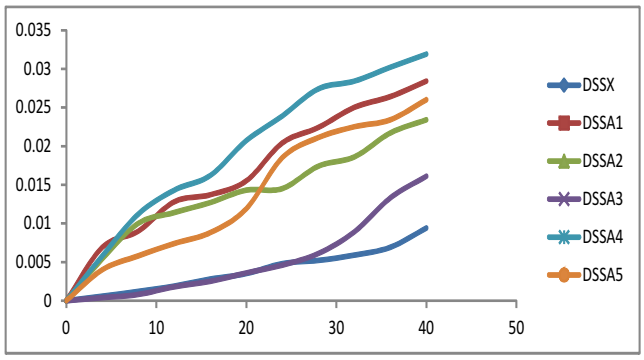

Figure 5: Gravimetric Corrosion Rate for 2205 ODS DSS composite in Pineapple juice Extract

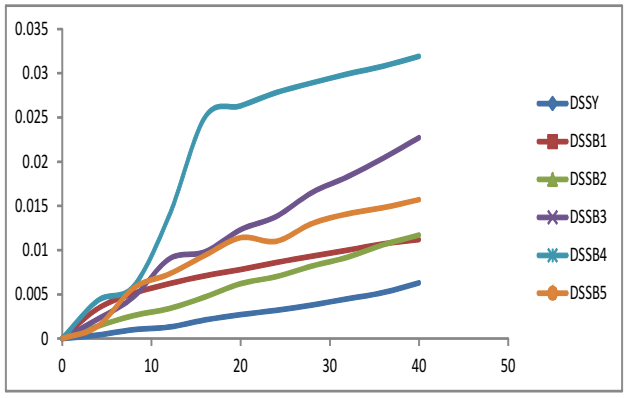

Figure 6: Gravimetric Corrosion Rate for 2507 ODS DSS composite in Pineapple juice Extract

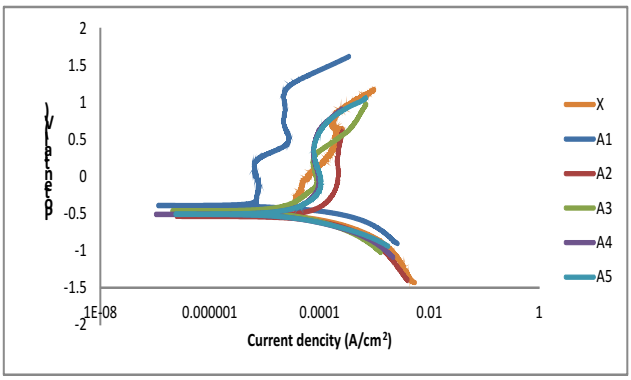

Figure 7: Polarization curves of ODS DSS 2205 composites in pineapple juice extract.

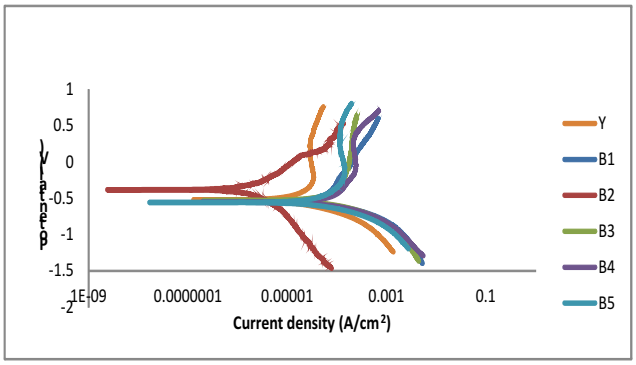

Figure 8: Polarization curves of ODS DSS 2507 composites in pineapple juice extract.

Figures 7 and 8 show the potentio-dynamic polarization scan for 2205 and 2507 composites respectively. From Figure 7, it was evident that introduction of PSZ alone to the as-received powders has shifted the corrosion potential to the more positive region (passive region) and decrease the corrosion current density which indicates a lower corrosion rate. This could be that the Cr present in the as-received was enough to convert the carbon to carbide thereby helping in the passivation of the composite in the pineapple juice extract. The same was not recorded when addition of Cr and Ni was included. It was expected that further addition of Cr and Ni should further shift the corrosion potential in the more positive region and cause a decrease in the corrosion current density but that was not the case. The reason can only be inadequate mixing of the participating powders to form the composites. However, A3 that has further increase in the quantity of PSZ, Cr and Ni has the second best corrosion resistance to the attack from the juice extract as indicated by the plot A3. Plots X, A4, A5, displayed almost the same corrosion potential but varying corrosion current density which explained the corrosion rate differences of the composites.

Table 5: Corrosion rate of ODS DSS 2205 composites in pineapple juice extract

Sample	ba (V/dec)	bc (V/dec)	Ecorr (V)(V)	icor (A/Cm3)	Icor (A)(A)	Cr (mm/yr)	Rp (Ω)
X	0.29073	6.2133	-0.53386	5.4961E-7	1.3696E-4	1.678E-3	8.6404E2
A1	0.27074	3.0161	-0.53858	6.4561E-7	1.4656E-4	2.007E-3	7.3618E2
A2	0.39767	-7.8545	-0.53283	8.6350E-7	2.0964E-4	2.522E-3	8.8898E2
A3	0.27079	1.3819	-0.46555	1.5732E-7	4.0064E-5	4.927E-4	2.4536E3
A4	0.21138	0.68923	-0.50841	1.4545E-7	3.704E-5	4.575E-4	1.8967E2
A5	0.19525	0.49229	-0.50246	1.2383E-7	3.1535E-5	3.9278E-4	1.9253E3

Figure 8 shows that introduction of PSZ alone slightly shifted the corrosion potential in the more negative region which means more corrosion rate; and the worst for these series. This could be that there was not enough Cr to help convert all the carbon to carbide. This was evident by further addition of Cr and Ni as shown in Table 2. This addition of 0.78 % Cr and 0.22 % Ni really help to shift the potential to the more positive region which helps to reduce the corrosion rate. However, B1, B3 and B4 have relatively equal potential, though different current densities which also explained the variation in the corrosion rate displayed by the various composites.

Table 6: Corrosion rate of ODS DSS 2507 composites in pineapple juice extract

Sample	ba (V/dec)	bc (V/dec)	Ecorr (V)(V)	icocc (A/Cm3)	Icor (A)(A)	Cr (mm/yr)	Rp (Ω)
Y	0.20663	0.80748	-0.52609	4.5708E-7	1.8283E-5	1.3924E-3	3.9083E3
B1	0.19948	4.7897	-0.546	3.6663E-7	8.3228E-5	1.1166E-3	9.9928E2
B2	0.57917	0.9577	-0.38491	1.6668E-8	4.2448E-6	5.0963E-5	3.6926E4
B3	0.41901	-0.82743	-0.53328	3.3775E-7	4.0511E-4	1.1104E-3	9.0866E2
B4	0.28001	-28.985	-0.55975	6.4787E-7	1.6499E-4	1.9513E-3	7.4426E2
B5	0.18632	0.5638	-0.56472	1.8121E-7	4.6148E-5	5.507E-4	1.3179E3

Also from the corrosion rate tables; Tables 5 and 6, it was evident that the ODS DSS composites of 2507 series displayed a relatively lower corrosion rate compared with those of 2205 composites. This was likely due to the general composition of the starting powder in which case, 2507 DSS has 24.8 % Cr, 7.72 % Ni and 0.025 % Al. while 2205 has lower percentage compositions of the above mentioned elements; 22.8 % Cr, 5.1 % Ni and 0 % Al. All these elements must have been responsible for the disparities in their corrosion rate values.

CONCLUSION

The final microstructures of the composites were found to be a function of the reinforcement and alloying elements. Addition of PSZ was found to have influenced the grains arrangement and invariably reduced the corrosion resistance of the composites. This PSZ addition must therefore be accompanied by addition of Cr and Ni to positively affect the electrochemical behaviour of the ODS composite. However, higher corrosion rate could also be linked to inadequate mixing of the starting powders, since there was enough Cr to convert the carbon to carbide but yet higher corrosion rate was recorded.

REFERENCES

Chawla N., Chawla K.K. 2006. Metal matrix composites. *New York, Springer.*

Chen H., Li Y.Y., Liu Y.B., Cao X.J. 2007. Influence of chromium on microstructure and sintering properties of FeNiMoCu system prealloyed powders. *Journal of Materials Processing Technology*, 182: 462-468.

Chen, W. and Zhou, J. (2009) Preparation and Characterization of Stainless Steel/TiC Nanocomposite Particles by Ball-milling Method, *Journal of Wuhan University of Technology-Mater.*38-41

Garcia C., Martin F., De Tiedra P., Garcia C. L., (2007) Pitting corrosion behavior of PM austenitic stainless steels sintered in Nitrogen-hydrogen atmosphere. Corrosion Science, 49: 1718-1736.

Kim T.K., Bae C.S., Kim D.H., Jang J., Kim S.H., Lee C.B., Hahn D. 2008. Microstructural observation and tensile isotropy of an austenitic ODS steel. *Nuclear Engineering and Technology,* 40: 305-310.

Lakhtin Y.(1987) Physical Metallurgy and Heat Treatment, 2nd Edition *MIR PublisherMoscow*.

Liu N.B., Lim S.C., Lu L., Lai M.O. (1994) Recent development in the fabrication of metal matrix-particulate composites using powder metallurgy techniques, *Journal of Materials Science,* 29, 1999-2007

Molins, C., Bas,J. A. and Planas, J. (1992) PM stainless steel: types and their characteristics and applications, *Advances in Powder Metallurgy*, 2(5),345–57

Muthupandi V., Srinivasan P.B., Shankar V., Seshadri S.K., Sundaresan S. 2005. Effect of nickel and nitrogen addition on the microstructure and mechanical properties of power beam processed duplex stainless steel (UNS 31803) weld metals. *Materials Letters,* 59: 2305-2309.

Obadele B.A., Ige O.O., Olubambi P. (2017), Ti-Ni-ZrO2 Fabrication and Characterization of Titanium-

Nickel- Zirconia Matrix Composites Prepared by Spark Plasma Sintering, Journal of Alloys and Compounds, 710, PP 825 – 830.

Olaniran O., Olubambi P.A., Potgieter J.H. and Adewuyi B. (2012), Influence of Cr – Ni Addition on porosity and Microstructure of $Z_rO_2(Y_2O_3)$ Dispersed Duplex Stainless Steel Composite, *Journal of Materials Science and Technology*; Vol.20, No. 2, PP 124 – 132

Olaniran O., Olubambi P.A., Potgieter J.H., Olaniran B., Adegbola A. and Folorunso D, (2013), Corrosion Behaviour of PM ODS composite sintered in Argon Atmospere, *Journal of Materials Science and Technology*; Vol.21, No. 3, PP 186 – 193 .

Olaniran O., Alaneme K., Obadele B.A., Folorunso D., Aribo S., Olanrewaju S. (2017), Structural Characterization of degradation of ODS Composite using SEM and XRM Techniques, Leonardo Electronic Journal of Practices and Technology; 30, 299 – 314.

Padmavathi, C., Upadhyaya, A. and Agrawal, D. (2007) Corrosion behavior of microwave- sintered austenitic stainless steel composites, *Scripta Materialia,* 57, 651–654.

Reddy K.M., Mukhopadhyay A., Basu B. 2010. Microstructure-mechanical-tribological property correlation of multistage spark plasma sintered tetragonal ZrO_2, *Journal of the European Ceramic Society,* 30: 3363 –3375.

Wei, D., Dave, R. and Pfeffer, R (2002) Mixing and characterization of nanosized powders: An assessment of different techniques, *Journal of Nanoparticle Research*, 4,21-41

Younesi M., Bahroloom M.E. 2010. Optimization of wear resistance and toughness of hydroxyapatite nickel free steel new bio-composites for using in total joint replacement. *Materials and Design,* 31: 234 - 243

FUTA JEET Vol 12 Issues 1&2 December, 2018

Journal of Engineering and Engineering Technology

ISSN 1598-0271

School of Engineering and Engineering Technology,
The Federal University of Technology, Akure, Nigeria

Journal of Engineering and Engineering Technology

A Multi-objective Resource-constrained Project Scheduling Problem Using Genetic Algorithm

'Ladi Ogunwolu, Adeyanju Sosimi and Toheeb Salahudeen

Department of Systems Engineering, Faculty of Engineering, University of Lagos, Nigeria.

A B S T R A C T

Keywords: Multi- Objective, Resource-Constrained, Project Scheduling Problem, Genetic Algorithm, Precedence relations.

Resource-Constrained Project Scheduling Problem (RCPSP) has been modeled as a single or multi-objectives, using minimization of project make-span, lateness, total weighted start time, total project cost and maximization of project net present value. In this paper, a multi-objective RCPSP incorporated resource idleness into the list of RCPSP objectives. Here, the RCPSP is modeled as a Mixed Integer Non-Linear Programme to depict the various objective factors namely cost, time and resource idleness. Genetic algorithm (GA) meta-heuristic solution technique is used to promote solution diversity and determine the Pareto optimal for the multi-objective problem. The performance of the proposed RCPSP model was evaluated using a standard test problem that consist of 5 activities, 3 reusable resource types and a network diagram; a comprehensive computational experiment was performed and the results were analyzed with precedence relations considering the objectives as single objectives, bi-objectives and in combined form as multi-objectives simultaneously. The integration of resources idleness into the multi-objective policy gives more realistic result.

1. Introduction

Resource-constrained project scheduling problem (RCPSP) remains a challenge to project managers in contemporary manufacturing, production planning, project design and the like; it has continued to attract a growing attention from researchers and project management experts, searching for enhanced solution techniques (Koulinas et al. 2014; F. Habibi e*t al*., 2018). RCPSP involves non-preemptive scheduling of project activities so that either the lead lag precedence relationships or resource constraints is not violated for optimal cost and time considerations. Hence RCPSP is NP-hard. A number of optimization techniques have been developed for solving the RCPSP depending on scale of project instances (Salem and Hassine, 2015; Abdolshal, 2014). Previous researches on RCPSP have focused on the development of RCPSP variants based on the original RCPSP formulation such as multi-mode problem formulation in which activities can be performed in several ways (Messelis and De Causmaecker, 2014), single-mode, pre-emption and non-pre-emption of activities, with reusable and non-reusable resources, single objective and multi-objective, multi project in which resources can be shared among several projects (Ma *et al*., 2016) etc. The single objective variant is sufficiently explored in literature (Hartmann and Briskorn, 2010). However, many real-world decision making problems often compels a tradeoff among many design considerations that gives rise to a set of Pareto-optimal solutions (Choi *et al.*, 2017). The exact procedure of seeking such a solution is known as multi-objective modeling (Martínez-Iranzo *et al*., 2009). The number of probable multi-objective formulations for the RCPSP is largely dependent on the choices made by project professionals hence, countless number of conflicting objectives have been reported (Al-Fawzan and Haouari, 2005) and objectives of critical concern to

Correspondence: 'Ladi Ogunwolu; fogunwolu@unilag.edu.ng
1fogunwolu@unilag.edu.ng, 2azeezadeyanju@gmail.com, 3salahudeentoheeb@gmail.com

decision managers and researchers, include the following: minimization of the project makespan; earliness or lateness; total project costs, resources availability costs; minimization of the total weighted start time of the activities; minimization of the number of tardy activities and maximization of the project net present value (Ballestín and Blanco, 2015).

Early research work on multiple objective RCPSP were premised on exact solution techniques as presented in (Blazewicz *et al*., 1983; Mohring *et al*., 2003; Mejia *et al*., 2017). The RCPSP was modeled as linear goal programming (LGP) model. Wieters (1979) presented an Integer Goal Programming (IGP) formulation to address multiple project scheduling problems competing for the same resources (i.e. renewable and non-renewable resources). In a related work, Slowinski (1989) presented a specialized optimization procedure for the multiple objective RCPSP, the algorithm creates all non-empty and different resource feasible subsets which do not violate the resource constraints. Both one-stage and two-stage multi objective linear programming (MOLP) methods were used to solve the problem. Palacio and Larrea (2016) formulated the RCPSP as a two Mixed-Integer Programming problem and used the exact solution technique to determine the optimal schedule. The first model was to minimize completion time of project, while the second maximizes the scheduling robustness. Several variants of the exact technique to RCPSP exist till date (Brucker *et al*., 1999; Kolisch and Padman 2001). However, the exact approach can only solve small scale problem instances in a satisfactory manner (Zhu *et al.*, 2006). Also, the exact algorithm requires several computations and as a result, they are slow to converge. Therefore, heuristic and metaheuristic solution procedures remain the only feasible way to obtain near optimal solutions for practically large resource-constrained project scheduling problems (Koulinas *et al*., 2014). Due to the computational complexity of the RCPSP, according to Thomas and Salhi (1998), the metaheuristic methods perform best in solving the resource constraint problem. Instead of whole space problem solution, a part of it is searched such that a good approximate solution is obtained at reasonable exponential time.

Several metaheuristic approaches have been reportedly developed to solve the RCPSP (Van Petegham and Vanhoucke, 2014). These include the Tabu Search (Yagiura and Ibaraki, 2001), the Pareto Simulated Annealing (PSA), the Genetic Algorithm (GA) (Mendes *et al*., 2009; Afshar-Nadjafi et al., 2013; Xhu *et al.*, 2017), Ant Colony Optimization (Li and Zhang, 2013) and hybrid algorithms (Myszkowski *et al*., 2015). Due to the successes recorded on the use of metaheuristics methods, the multi objective RCPSP formulation in this study will be solved using Genetic Algorithm (GA).

In this paper, a multi-objective RCPSP with synchronized conflicting objectives of Make-span, Total Cost and Resource Idleness minimization is proposed for the first time. The modeling technique is premised on hybrid of exact and meta-heuristic approaches.

2. The Model

2.1 Problem Description

A model was formulated for the RCPSP. The model consists of three objectives which made the RCPSP multi-objective in nature. The objectives are to minimize the project cost, project duration and resource idleness. The following assumptions were made in the development of the model: (1) Preemptive activities: once an activity is ongoing, it cannot be interrupted (2) Reusable resources: The resource types are reusable after a prior use (3) The project was funded via loan at some interest rate. (4) Deterministic approach is used.

2.2 Model Development

Let G = (V, A) represent a direct acyclic graph (project scheduling is usually represented by a direct acyclic graph), where the set of nodes V = {1, 2,…, n+1} represents activities in the project and the set of arcs (i, j) ∈ A with precedence link between activities

Let $G = (V, A)$ represent a direct acyclic graph (project scheduling is usually represented by a direct acyclic graph), where the set of nodes $V = \{1, 2, \ldots, n+1\}$ represents activities in the project and the set of arcs $(i, j) \square A$ with precedence link between activities i and j such that,

$$f_{ij} = \begin{cases} 1 & \text{if activity } i \text{ immediately precedes } j,\ i \neq j \\ 0 & \text{otherwise} \end{cases}$$

So, if C_{i0} is the initial cost, x_i the start time and t_i, the duration of execution of activity i of the project, $i = 1, 2, \ldots, n$ and let r be the uniform compound interest rate of loan and $\overline{T}_s$ the cumulative time horizon of the loan procured up to the beginning of the current activity (T_s) at time segment s, $s = 1, 2, \ldots, S$. the actual cost of executing the activity is,

$$\overline{C}_i = f_{ij} C_{i0} (1 + r)^{[(\overline{T}_s + \tau_s - x_i)]}$$

Similarly, if $\theta(q)$ is the quantity of resource type q available for project execution, $q = 1, 2, \ldots, Q$ and defining two binary parameters,

$$R(i, q) = \begin{cases} 1 & \text{if activity } i \text{ uses resource type } q \\ 0 & \text{otherwise} \end{cases}$$

$$P(i, j) = \begin{cases} 1 & \text{if } i \text{ is an immediate predecessor of } j,\ i \neq j \\ 0 & \text{otherwise} \end{cases}$$

the resource idleness function of the model can be modeled as,

$$\sum_{q=1}^{Q} \{ \theta(q) x_n - \sum_{i=1}^{n} [R(i, q) t_i N(i, q)] \}$$